Spectroscopic Study of Nonamphiphilic 2,2′-*p*-Phenylenebis(5-phenyloxazol) (POPOP) Assembled in Supramolecular Langmuir−Blodgett Films

A. K. Dutta[†]

Department of Spectroscopy, Indian Association for the Cultivation of Science, Jadavpur, Calcutta 700 032, India

Received: June 6, 1996; In Final Form: September 10, 1996[⊗]

This paper reports the incorporation of a nonamphiphilic blue laser dye 2,2′-*p*-phenylenebis(5-phenyloxazol), abbreviated as POPOP, in Langmuir−Blodgett (LB) films mixed with stearic acid (SA) and their spectroscopic properties. The surface pressure versus area per molecule isotherms of POPOP mixed with SA at different molar ratios reveal a plateau-like region that suggests reorientation of the POPOP molecules from lying flat at the air−water interface to an almost vertical alignment. Miscibility studies indicate a repulsive type of interaction between the components in the mixture, resulting in the formation of microcrystallites in the LB films that is confirmed by spectroscopic studies. Perhaps the most interesting feature of this study is the appearance of a new band at about 400 nm in absorption spectra of the mixed LB film of POPOP and SA that is assigned to a low-lying hidden ^1L_b state. The appearance of the same band in a mixture of ethanol and water with the volume fraction of water in the mixture exceeding 76% confirms that the manifestation of this band is aggregation induced. Fluorescence emission studies of POPOP in solution reveal a structured emission that originates from the ^1L_a state, while the emission studies from the LB films exhibit two bands, one at 420 nm originating from the low-lying ^1L_b state of the monomer and the other at 460 nm corresponding to a ^1L_b dimer. Excitation and polarized anisotropy measurements confirm these findings and indicate that the above observations may be attributed to a deformed geometry of the POPOP molecules in the LB films.

Introduction

Organized ultrathin films prepared by the Langmuir−Blodgett (LB) technique[1] offers the simplest yet the most elegant method of obtaining highly organized supramolecular assemblies, the optical and electronic properties of which may be manipulated with ease. In recent years, considerable attention has been focused on the study of new chromophores and dyes incorporated in supramolecular LB films to satisfy specialized needs such as high photorefractivity,[2] photoconductivity,[3] and large nonlinear optical responses[4] that are deemed to be important in the design of photonic devices.[2−5] Phenyl and oxazole based laser dyes constitute an important class of blue-light-emitting materials that meet some of these requirements and have been recently studied in composite glasses[6] and polymer films[7] and have been used as an active material in polymer-based electroluminescent devices and thin film light-emitting diodes (LED's).[8]

2, 2′-*p*-Phenylenebis(5-phenyloxazol) abbreviated as POPOP is a well-known oxazine dye characterized by its intense fluorescence[9] in the blue region of the visible spectrum and used in scintillators, solar energy concentrators,[9c] and recently, thin film electroluminescent devices.[8] Despite such interesting properties, nonamphiphilic POPOP has never been studied in LB films. Nonamphiphilic molecules mixed with fatty acids form excellent LB films,[1,10,11] and recent studies[10−13] have suggested that the behavior of nonamphiphilic molecules is quite similar to their amphiphilic counterparts especially with regard to their spectroscopic and aggregating properties. These similarities justify the study of nonamphiphilic compounds in mixed LB layers, since they may be readily put to large scale applications that are cost effective compared to their amphiphilic counterparts, which are usually difficult to synthesize and expensive.

This paper reports for the first time the behavior of the mixed films of nonamphiphilic POPOP and SA at the air−water interface and their spectroscopic properties when transferred on to quartz substrates as LB films. The chief interest in this molecule stems from the fact that the oxazole and phenyl rings may undergo rotation about the other that is likely to produce large changes in their electronic states and hence their spectroscopic characteristics that may reflect the interaction between the molecules and their microenvironment. Hence, such molecules in addition to their manifold applications may serve as potential molecular probes in establishing a spectra−structure−property relation for such molecules assembled in constrained media or systems representing restricted geometries such as LB films.

Experimental Section

POPOP was a product of Aldrich Chemical Co., Milwaukee, WI, and used without further purification. The purity of the sample was, however, checked by thin layer chromatography, as well as by absorption and emission spectra of POPOP in solution, and was found to be in good agreement with reported data.[9] Stearic acid (SA) was purchased from Sigma Chemical Company, St. Louis, MO, and used without further purification. A commercially available alternate layer Langmuir−Blodgett deposition trough, Joyce-Loebl trough 1V obtained from Joyce-Loebl Inc., Newcastle upon Tyne, U.K., was used for the deposition of mono- and multilayers. The subphase used was doubly distilled water deionized by a Mill-Q plus water purification system. The pH of the subphase was 6.3 in equilibrium with atmospheric carbon dioxide, and its resistivity was 18.2 MΩ cm. A Joyce-Loebl water refrigerating system

[†] Present address: Dr. A. K. Dutta, Centre de Recherche en Photobiophysique, Université du Québec a Trois-Riviéres, Trois-Riviéres, Québec, Canada G9A 5H7. Fax: +1 (819) 376 5057.

[⊗] Abstract published in *Advance ACS Abstracts,* December 15, 1996.

S1089-5647(96)01671-9 CCC: $14.00

was used to maintain constant temperature of the subphase at 15 °C with an accuracy of 0.1 °C. Surface pressure measurements were achieved by a filter paper Wilhelmy plate that was interfaced to a microcomputer that also controlled the moving barrier and maintained constant pressure at the air−water interface with an accuracy of 0.1 mN/m. The surface pressure versus area per molecule isotherms were obtained by spreading about 100 μL of a chloroform solution of stearic acid and POPOP mixed in a predetermined ratio, and after sufficient time for the solvents to have evaporated, the film at the air−water interface was compressed very slowly at a rate of 5×10^{-3} nm^2 mol^{-1} s^{-1}. The average area per molecule was calculated by dividing the total surface area occupied by the floating monolayer by the total number of molecules in the monolayer at any given surface pressure. Each isotherm was obtained by averaging four or five runs, and reproducibility was checked to be well within a permissible experimental error limit of 5%. Y-type deposited mono- and multilayers of the mixed films of POPOP and SA on fluorescent grade quartz slides were obtained by moving the slides vertically through the floating monolayer very slowly at a rate of 1 mm/s at a constant surface pressure of 25 mN/m. The transfer ratio of the POPOP molecules was calculated from the ratio of the area of the substrate coated with the monolayer to the actual decrease in the surface area of the floating monolayer at the air−water interface and was found to be 0.98 ± 0.01 for Y-type deposition on quartz slides.

Absorption spectra of the dye in solution and in the LB films were recorded on a Shimadzu UVPC-2010 absorption spectrophotometer, and emission was recorded on a Perkin-Elmer MPF-44A emission spectrofluorometer. The emission spectra of LB films were obtained by front face excitation by placing the films in suitable holders that held the film at an angle of 45° to the source and detector. Narrow band-pass filters (5 nm) were used to minimize the effects of scattering and reabsorption. Polarized emission and excitation spectra were recorded by introducing polarizers in the path of light between the source and sample and also between the sample and detector.

Results and Discussion

Study of Mixed Films of POPOP and SA at the Air−Water Interface. To study the behavior of pure POPOP at the air−water interface, 100 μL of a solution of pure POPOP in chloroform (1×10^{-3} M) was spread at the air−water interface and then compressed at a rate of 5×10^{-3} nm^2 molecule^{-1} s^{-1} after allowing the solvents to evaporate. It was observed that the surface pressure of the pure film showed a sharp rise from an initial "zero" value to about 5 mN/m at which it remained constant despite a large decrease in the average area per molecule from 0.7 to 0.2 nm^2, as evident from Figure 1g. Further compression resulted in a steep isotherm, indicating the attainment of a solid condensed phase. However, all attempts to transfer the monolayer of pure POPOP from the air−water interface onto the solid substrates failed despite a steep isotherm and an extremely stable area per molecule versus time curve (figure not shown). Mixing POPOP with SA yielded highly transferable mono- and multilayers that could be transferred onto quartz substrates with a transfer ratio of about 0.98 ± 0.01.

Figure 1 shows the surface pressure (Π) versus area per molecule (A) isotherms of pure POPOP mixed with SA at different molar ratios. The $\Pi-A$ isotherms of the mixed films of POPOP and SA replicate the isotherm of pure POPOP with the only difference being that the flat plateau-like region shortens in length with increasing mole fraction of SA in the mixture. Very likely, this plateau indicates a phase transition corresponding to a reorientation of the POPOP molecules from lying flat

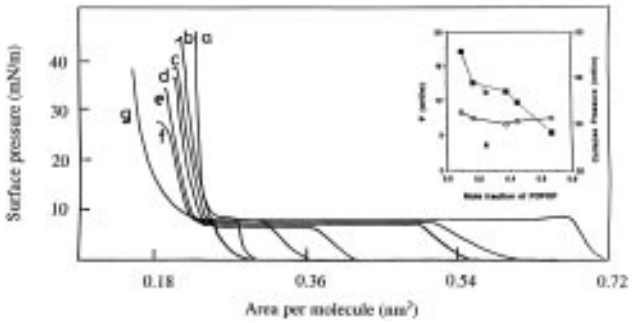

Figure 1. Surface pressure versus area per molecule isotherms of mixed films of POPOP and SA at different mole fractions of POPOP: (a) 0; (b) 0.09; (c) 0.17; (d) 0.38; (e) 0.47; (f) 0.67; (g) 1.00. Inset shows (a) the plot of the surface pressure corresponding to the plateau region of the isotherm versus the mole fraction of POPOP and (b) the plot of the collapse pressure versus the mole fraction of POPOP.

at the air−water interface at low surface pressures to an almost upright vertical alignment of the POPOP molecules with its long axis perpendicular to the air−water interface at high surface pressures. These features seem to be characteristic of POPOP and sharply in contrast to other similar molecules, namely, the polyphenyls[14] and oligothiophenes.[15] Other molecules, namely, the cyanobiphenyls,[16] polyglutamates,[17] pentadecanoic acid,[18] hexadecanoic acid,[19] and their esters also show similar plateau-like regions in their isotherms that are often interpreted in terms of phase transition brought about by large changes in their molecular orientation and arrangement or multilayer and aggregate formation. Moreover, the small area per molecule of the mixed films of POPOP and SA at large surface pressures suggests that the POPOP molecules stand on their edge vertically with their long axis almost parallel to the normal on the air−water interface and sandwiched as aggregates between SA chains, which appears to be consistent with the behavior of other linear rod-like molecules.[14,15] The average area per molecule of the mixed monolayer of POPOP and SA was observed to decrease with increasing mole fraction of POPOP in the monolayer, and it was thought that the POPOP molecules probably submerged below the air−water interface. Spectroscopic analysis of small aliquots of water samples sucked out from just below the floating layer using a bent tube and method that is described in detail elsewhere[14] failed to indicate the presence of POPOP in the subphase. These results indicated that the POPOP molecules were not submerged below the air−water interface but sandwiched between the SA chains and also very likely squeezed out of the monolayers onto their surface. Identical results have been reported for other linear molecules.[14−15] Interestingly, these results are sharply in contrast with the findings by Kramarenko,[20] which indicated that amphiphilic oxazole dyes indeed lie flat with their long axis parallel to the air−water interface.

Information on the miscibility of the components in mixed monolayers may be obtained from the $\Pi-A$ isotherms using the surface phase rule.[21] The lower curve (marked a) in the inset of Figure 1 shows a plot of the surface pressure corresponding to the plateau-like region versus the molar concentration of POPOP in the mixed film of POPOP and SA. Within the limits of experimental error the surface pressure is found to be independent of the molar composition of the mixed film, which indicates that very likely POPOP and SA molecules are immiscible at all possible compositions at that surface pressure. This seems justified in view of the completely different molecular structure and chemical characteristics of the components.[22] The upper curve (marked b) in the inset of Figure 1 corresponds to a plot of the collapse pressure at low areas per molecule versus the mole fraction of POPOP in the mixed film.

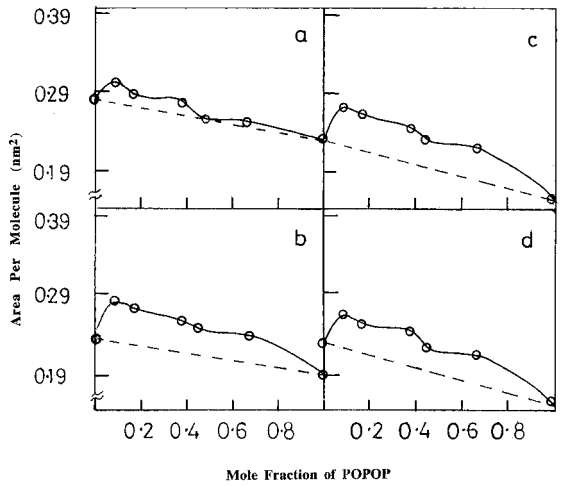

Figure 2. Plot of the average area per molecule of the mixed film versus the mole fraction of POPOP at the air−water interface at different surface pressures: (a) 10, (b) 15, (c) 20, and (d) 25 mN/m.

It is evident from the figure that the collapse pressure decreases with increasing mole fraction of POPOP, which suggests that at high surface pressures the components of the mixture, despite their differences in chemical and physical properties, are at least partially miscible, although the same components tend to be completely immiscible at low surface pressures.

Figure 2 shows the plot of the average area per molecule versus mole fraction of POPOP in the mixed films at the air−water interface at different constant surface pressures. The dotted line in the figure represents the ideality curve that corresponds to the additivity rule[21] for a noninteracting two-component system. In such a system the average area per molecule is given as

$$A_{12} = N_1A_1 + N_2A_2$$

where N_1 and N_2 are the mole fractions and A_1 and A_2 are the areas per molecule of the first and second components of the mixture, respectively. Interestingly, all the curves show a positive deviation from the ideality behavior that is indicative of a repulsive interaction between the components, suggesting aggregation in the mixed films even at low concentrations and low surface pressures, which is consistent with the behavior of other nonamphiphiles.[11,14]

Although interactions between molecules in the mixed films at the air−water interface is extremely complex, a qualitative explanation, however, seems possible. Although the interactions between the SA and POPOP molecules with the water surface tend to orient the molecules at the air−water interface, the SA−SA, POPOP−POPOP, and SA−POPOP interactions determine the spatial distribution of the moieties in the monolayers. Although the weaker SA−POPOP interaction tends to make the components miscible, which tends to produce a homogeneous distribution of the constituing moieties in the monolayer, the SA−SA and POPOP−POPOP, which are much stronger, favor the formation of 2D and 3D aggregates[12,23] of the pure components, and this has been confirmed by fluorescence microscopy[13] and Brewster angle microscopy.[23]

Steady-State Absorption and Emission Spectra of POPOP in Solution, LB Films, and Ethanol−Water Binary Solvent Mixture. Figure 3 shows the absorption spectra of POPOP in ethanol (1×10^{-5} M) and 10 layers of a mixed film of POPOP and SA (1:20). The solution absorption spectrum in the 300−450 nm region shows distinct bands at 342, 358, and 376 nm that corresponds to the ^1L_a transition of the POPOP molecule and is directed parallel to the long axis of the molecule.[9b] The

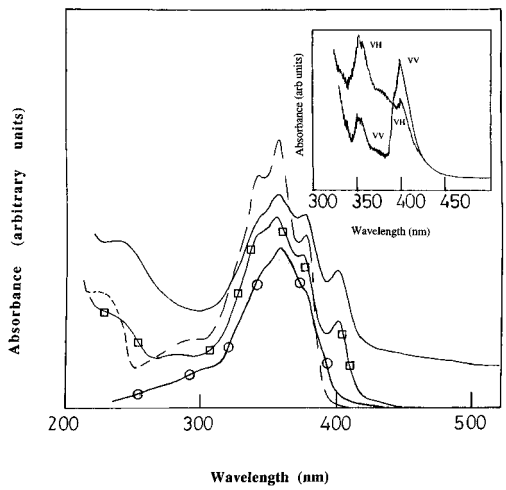

Figure 3. Absorption spectra of POPOP in solution (dashed line), PMMA film (open circles), binary mixture of ethanol (15%) and water (85%) (open squares), and LB films (continuous line). Inset shows the polarized absorption spectra of the mixed films of POPOP and SA. VV and VH indicate polarization in a direction parallel to or perpendicular to the dipping direction.

LB film absorption spectrum also shown in the same figure appears to be identical with the solution absorption spectrum except that in addition to an overall broadening of the spectral profile a new absorption band appears at 400 nm. This band at 400 nm does not seem to bear a one-to-one correspondence with the absorption bands in solution and its origin does not seem to be readily explicable. Broadening of the absorption profile indicates aggregation. According to the intermediate strength exciton coupling theory,[24a−c] dipole−dipole interaction results in the raising or lowering of the exciton band to a position either energetically higher or lower than the monomer band. Such a change in energy is given by $\Delta E = 2\mathbf{M}^2(1 - 3\cos^2\theta)$-$(1 - 1/N)/\mathbf{r}^3$ where $\mathbf{M}$ is the dipole moment vector, N is the number of monomers in the aggregate, θ is the angle between the dipole moment of the molecule and the $\mathbf{r}$ vector that joins the centers of the two dipoles. When $0° < \theta < 54.7°$, the exciton band is located below the monomeric band that causes a red shift and the corresponding aggregates are referred to as the J-aggregates,[24d−g] while for $54.7° > \theta > 90°$ the exciton band is located above the monomer band that causes a blue shift and the aggregates are referred to as H-aggregates.[24f−h] Corresponding to the magic angle $\theta = 54.7°$, the shift observed is zero and independent of N and $\mathbf{r}$ and the aggregates are referred to as the I-aggregates.[24i−j] The broadening of the ^1L_a absorption bands accompanied with no shift seems to suggest the formation of I-aggregates in the LB films where the long axes of the neighboring POPOP molecules are parallel to each other and makes an angle of 54.7° with the vector joining the centers of the POPOP molecules, and this is also consistent with the results obtained from the $\Pi-A$ isotherm measurements.

As mentioned earlier, the origin of the band at 400 nm is not readily explicable. Several possibilities exist: (a) a long wavelength component produced as a result of exciton splitting; (b) a dimer band; (c) a low-lying band corresponding to the ^1L_b state. The fact that the ^1L_a bands in solution and in the LB films show no shift relative to each other with regard to their band positions rules out the possibility of the band at 400 nm being the long wavelength component produced as a result of an exciton band splitting. The second possibility of this band being a dimer band seems justified, since a close approach of these moieties due to aggregation in the LB films may generate such dimeric species. An estimate of the full width at half-maximum (fwhm) of the bands at 400 and 376 nm revealed

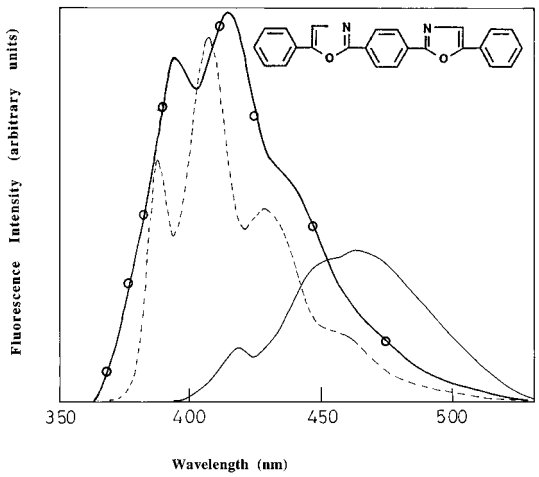

Figure 4. Emission spectra of POPOP in solution (dashed line), PMMA film (open circles), and LB films (continuous line). λ_{exc}= 300 nm. Inset shows the molecular structure of POPOP.

that the fwhm of the band at 400 nm was 0.3 times the fwhm of the band at 376 nm. This indicated that very likely the band at 400 nm is not a dimeric band, since such bands are expected to be broad and have a large fwhm. Using the relation[25]

$$f = 4.3 \times 10^{-9} \int \epsilon \, d\nu = 4.3 \times 10^{-9} \epsilon_{max} (\Delta\nu)_{1/2}$$

the ratio of the oscillator strengths at 400 and 376 nm was estimated to be about 0.16, where ϵ_{max} is the molar extinction coefficient at the absorption band maximum and $(\Delta\nu)_{1/2}$ is the fwhm of the same absorption band under consideration. The small value of the oscillator strength of the band at 400 nm compared to that at 376 nm indicated that the origins of the two bands were different. Polarized absorption studies shown in the inset of Figure 3 indicated that although the band at 400 nm is polarized parallel to the dipping direction, the band at 376 nm is polarized in a direction perpendicular to the dipping direction. These results confirm that the band at 400 nm is indeed the low-lying ^1L_b band and is also consistent with the suggested orientation of the POPOP chromophores in the LB films as suggested by the $\Pi-A$ isotherm measurements. In addition, the low quantum yield of fluorescence of POPOP in the LB films, as will be discussed in a later section of this paper, confirms that indeed the band at 400 nm is the ^1L_b band.

To elucidate better the role of aggregation, the absorption spectra of POPOP incorporated in a poly(methyl methacrylate) (PMMA) matrix and in binary solvent mixtures of ethanol and water were also studied as shown in Figure 3. Interestingly, it was observed that in PMMA the absorption spectrum of POPOP resembled the solution absorption spectrum and the low-lying band at 400 nm was never obtained irrespective of the concentration of the dye in the polymer. The absorption spectrum of POPOP in the binary solvent mixtures of ethanol and water was also studied. The absorption spectra of POPOP in the binary solvent mixtures with volume fraction of water less than 0.76 were found to be identical with that in pure ethanol. However, when the volume fraction of water in the mixture exceeded a threshold limit of 0.76, the band at 400 nm was readily revealed as shown in Figure 3.

Figure 4 shows the emission spectra of POPOP in ethanol (1×10^{-5} M) and in the mixed LB films with SA. The fluorescence emission spectrum in ethanol solution shows bands at 338, 407, 428, and 458 nm that are in excellent agreement with reported data.[9] The excellent mirror symmetry between the absorption and emission bands in solution, the high quantum yield of fluorescence (ϕ = 0.93), and the short fluorescence lifetime (τ =1.3 ns) suggest that the POPOP molecules behaves as a rigid rod where the phenyl rings and the oxazole rings are coplanar and undistorted in the excited state. Figure 4 also shows the emission spectrum of 10 layers of the mixed LB film of POPOP and SA. The emission spectrum consists of a weak band at about 420 nm and a relatively intense band in the 430−550 nm region centered at about 460 nm. The fluorescence emission from the mixed LB films of POPOP and SA was found to be extremely weak (ϕ = 0.02) compared to that in solution. Such a weak fluorescence from the mixed LB films as well as the 0−0 of the emission band located at about 420 nm confirms that emission originates from the lowest ^1L_b state. The broad band centered at about 460 nm may be attributed to the aggregated species that probably corresponds to a dimer of POPOP. In fact, the red-shifted and extremely broad and structureless profile of the emission band supports such a conclusion. Indeed, oxazoles are known to exhibit weak excimeric emission[26] and have been reported for several oxazoles, although excimer formation is unfavorable as demonstrated by the theoretical calculations of Lami.[27] Interestingly, however, excimeric emission from short oxazole derivatives has been observed when they are incorporated in constrained media such as cyclodextrins.[26c−d] Dissolution of the LB films in ethanol reproduced the intense fluorescence emission spectrum, confirming that the observed effects did not arise from impurities or artifacts.

In this context, it must be pointed out that a complete understanding of the exact mechanism that causes the manifestation of the low-lying ^1L_b bands in POPOP is not fully understood. However, the remarkable structural similarity of POPOP with the polyphenyls suggests that the processes involved in POPOP and the polyphenyls are very likely similar. In polyphenyls the low-lying ^1L_b band is never observed, but in the LB films they are readily manifested.[14] The manifestation of this band has been attributed to a small deformation of the molecular structure, caused by such influences as mechanical pressure, thermodynamic and geometrical compatibility for packing of the moieties in the aggregates, that actually controls the balance between the inter- and intramolecular forces and determines the relative orientation of the various rings in the polyphenyl. X-ray diffraction, differential scanning calorimetric studies, and theoretical calculations support such deformations.[28] Recent studies by Doroshenko[29] have provided evidence that substitution and deformation of the molecular structure result in large changes of the charge distribution in the molecules that causes large shifts in the absorption and emission bands of oxazoles. Given these results and the above-mentioned facts, it does not seem unreasonable that owing to mechanical pressure exerted on the molecules during compression and their interaction with the local environment in the LB films and to geometrical and thermodynamical requirements during the formation of aggregates, a deformation of the POPOP molecule probably occurs. This is also feasible from the geometrical point of view, since the oxazole and phenyl rings are capable of rotating about the long axis of the molecules. Such small distortion of the molecules may cause forbidden transitions to become partially allowed, resulting in the manifestation of the low ^1L_b lying states and emission therefrom as discussed above.

Binary solvent mixtures are known to form organized aggregates.[30] In an effort to understand better the spectral characteristics of the aggregates, we have compared the fluorescence emission of POPOP assembled in LB films mixed with SA and POPOP in an ethanol−water binary mixture at different volume fractions of water in the mixture. Figure 5 shows the emission spectra of POPOP at different compositions

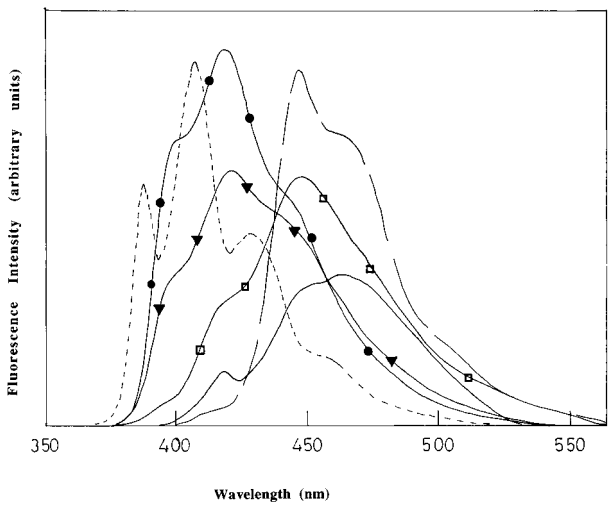

Figure 5. Emission spectra of POPOP in LB films (continuous line), microcrystals (broken line), and binary solvent mixtures of ethanol and water at different volume fractions of water in the mixture: (a) 0 (dashed line); (b) 0.2 (filled circles); (c) 0.6 (filled triangles); (d) 0.85 (open squares). λ_{exc}= 300 nm.

of the ethanol−water binary mixtures, LB films, and microcrystals. It is evident from the figure that the emission of POPOP in the binary solvent mixture corresponding to a volume fraction of 0.2 of water in the mixture closely resembles the emission in pure ethanol. With increasing volume fraction of water, the 0−0 band and the adjacent high-energy bands appear to get quenched while the low-energy bands show enhancement in their intensity. Such behavior is diagnostic of aggregation-induced reabsorption and has been reported for several molecules.[11d−g,14a,b] Despite the remarkable similarity in the molecular structure of the polyphenyls and POPOP, their spectroscopic characteristics in the binary solvent mixtures and in the LB films were found to be quite different. Although the polyphenyls incorporated in the LB films and in the binary solvent mixtures were identical and exhibited aggregated induced reabsorption effects,[14,31] the spectrum of POPOP in the LB films and in the binary solvent mixtures were completely different. The LB film emission spectrum of POPOP showed a broad and diffuse band with its maximum at 460 nm corresponding to the dimer, while that in the binary mixture corresponded to the aggregation-induced reabsorption spectrum. Clearly, the aggregates generated in the two systems are different. Interestingly, however, the absorption spectra of POPOP in the LB films and in the binary solvent solvent mixture were found to be identical and both manifested the band at 400 nm. These features clearly demonstrate the fact that the causes for the manifestation of the absorption band at 400 nm and the emission band at 460 nm are different and independent of each other. In addition, the emission spectra of POPOP microcrystals shown in Figure 5 are found to be different from the LB film emission spectra, which points to the fact that despite the formation of 3D microcrystallites in the mixed LB films of POPOP and SA, the molecular packing arrangement in each of the systems is different. Aggregation-induced reabsorption effects have been explained in terms of molecular distortion and phase transitions by several authors.[32] A plausible explanation seems to be that as a result of molecular aggregation, distortion of the molecular structure of POPOP occurs that results in unallowed or forbidden transitions becoming allowed, which is readily manifested as the low-lying ^1L_b band at 400 nm and emission therefrom. Close proximity of the distorted POPOP molecules in the aggregates formed in the LB films

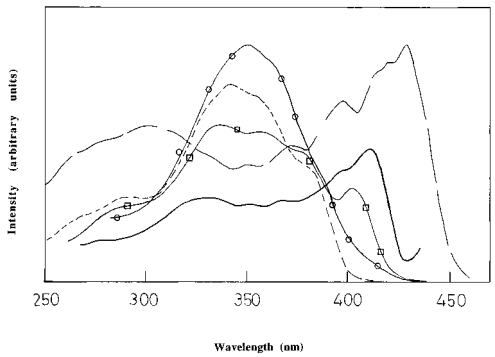

Figure 6. Excitation spectra of POPOP in ethanol (dashed line), binary solvent mixture with volume fraction of water of 0.85 (open squares), LB films (continuous line), PMMA films (open circles), and microcrystals (broken line). Emissions were monitored at the emission maxima in each case.

results in the formation of a ^1L_b dimer state that corresponds to the emission at 460 nm.

Spectroscopic Studies of the Excitation Spectra of POPOP in Solution, LB Films, and Ethanol−Water Binary Solvent Mixture. Figure 6 shows the excitation spectra of POPOP in ethanol and in the LB films obtained by monitoring the band maximum of the fluorescence emission. The excitation spectra of POPOP in ethanol shows the 0−0 band at 380 nm that is in good agreement with the ^1L_a band in solution. This is in fact expected, since the ^1L_a state is the lowest singlet state of POPOP in solution. The LB film excitation spectrum, on the other hand, shows two bands, one corresponding to the ^1L_a band around 380 nm and the other around 410 nm. The manifestation of this band confirms that in LB films the emission originates from the band at 410 nm corresponding to the ^1L_b state. This band is never manifested in PMMA matrix or in binary solvent mixtures with low volume fractions of water in the mixture but is readily manifested when the volume fraction of water in the mixture exceeds a threshold composition corresponding to 0.76 volume fraction of water in the binary mixture of ethanol and water. These results confirm that indeed the band at about 400 nm is an indicator of organized aggregates of POPOP and is the lowest ^1L_b band. The large differences observed between the excitation spectra of POPOP in solution and in the LB films confirm that the broad-band emission is not due to an excimer but to a dimer. Furthermore, the excitation spectra of POPOP microcrystallites formed in the LB films and those formed by recrystallization or in the binary solvent mixtures are found to be different and confirm that different molecular packing in the different crystallites, which seems justified as molecular packing in the crystals, are known to be largely dependent on the method of their preparation.

Figure 7 shows the polarized excitation spectra of POPOP assembled in the LB films mixed with SA. The continuous line corresponds to the VV polarization, while the dashed line corresponds to the VH polarization, where VV stands for polarization parallel to the dipping direction while VH stands for polarization perpendicular to the dipping direction. A careful examination of Figure 7 showed that although the transition dipole moment corresponding to the band at 410 nm has a larger component parallel to the VH direction, the transition dipole moment corresponding to the band at 380 nm has a larger component parallel to the VV direction. This confirmed that the bands at 410 and 380 nm were of different origin and polarization, which is again consistent with the polarized absorption studies.

The inset of Figure 7 shows the plot of the anisotropic ratio[33] versus the wavelength. The anisotropy ratio (r) is calculated

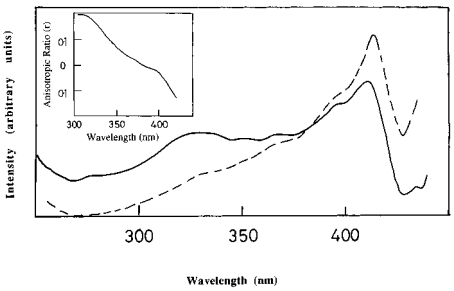

Figure 7. Polarized excitation spectra of the LB films of POPOP. Dashed line shows the VH polarization, while the continuous line shows the VV polarization. Inset shows the plot of the anistropic ratio (*r*) versus wavelength.

by the relation[33]

$$r = (I_{VV} - I_{VH})/(I_{VV} + 2I_{VH}) = 0.2(3\cos^2\theta - 1)$$

where I_{VV} and I_{VH} stand for intensities of polarizations parallel and perpendicular to the dipping direction of the substrate and θ is the angle between the absorption and emission dipole moments. At 410 nm the value of r is found to be -0.076, which yields θ equal to 55°, which suggests that absorption and emission occur from different electronic states. This is consistent with the fact that absorption occurs at both the ^1L_a and ^1L_b state, while emission occurs from the ^1L_b state of the monomers as well as from the ^1L_b state of the dimer.

Conclusions

In summary, nonamphiphilic POPOP mixed with SA forms excellent mono- and multilayers at the air−water interface that may be easily transferred onto solid substrates as LB films with a high transfer ratio. Detailed studies reveal that the POPOP molecules tend to lie flat at the air−water interface at low surface pressures but stand erect with their long axis perpendicular to the air−water interface at high surface pressures. Spectroscopic studies of the absorption spectra of the LB films show extensive broadening but no shift that indicates I-type aggregation. The presence of the band at 400 nm in the absorption spectra corresponding to the low-lying ^1L_b state indicates distortion of the POPOP molecules in the LB films. One possible reason seems to be that as a result of organized aggregation, small structural deformations of the molecules cause forbidden or weak transitions to become allowed, resulting in the manifestation of the low-lying ^1L_b state, which is confirmed by polarization studies. The emission spectra of the LB films of POPOP show two bands, one at 420 nm corresponding to the monomer fluorescence of POPOP from the ^1L_b state and the other a broad-band emission at 460 nm that originates from the ^1L_b dimer of POPOP. Anisotropy measurements suggest that both the absorbance and emission from POPOP occur from different electronic states, which confirms that absorption occurs at the ^1L_a and ^1L_b states but emission occurs from the ^1L_b state of the monomer and the dimer.

References and Notes

(1) Ulman, A. *An Introduction to Ultrathin Organic Films: From Langmuir-Blodgett Films to Self Assemblies;* Academic, New York, 1991.

(2) Nolte, D. D. *Photorefractive Effects and Materials;* Kluwer Academic Publishers: London, 1995.

(3) (a) Burghard, M.; Fischer, C. M.; Schmeizer, M.; Roth, S.; Hanack, M.; Gopel, W. *Chem. Mater.* **1995,** *7*, 2104. (b) Law, K. Y. *J. Phys. Chem.* **1988**, *92*, 4226.

(4) Prasad, P. N.; Williams, D. J. *Nonlinear Optical Effects in Molecules and Polymers*; John Wiley and Sons, Inc.: New York, 1991.

(5) Swalen, J. D.; Allara, D. L.; Andrade, J. D.; Chandross, E. A.; Garoff, S.; Israelachvili, J.; McCarthy, T. J.; Murray, R.; Pease, R. F.; Rabolt, J. F.; Wynne, K. J.; Yu, H. *Langmuir* **1987**, *3*, 932.

(6) Givish, R.; He, G. S.; Prasad, P. N.; Narang, U.; Li, M.; Bright, F. V.; Reinhardt, B. A.; Bhatt, J. C.; Dillard, A .G. *Appl. Spectrosc.* **1995**, *49*, 834.

(7) (a) Yang, Z.; Sokolik, I.; Karasz, F. E. *Macromolecules* **1993**, *26*, 1188. (b) Tachelet, W.; Jacobs, S.; Ndayikengurukiye, H. Geise, H. J. *Appl. Phys. Lett.* **1994**, *64* (18) 2364. (c) Hilberer, A.; Van der Brouwer, H. J.; Scheer, B. J.; Wildeman, J.; Hadziioannou, G. *Macromolecules* **1995**, *28*, 4525.

(8) (a) Greenham, N. C.; Moratti, S. C.; Bradley, D. D. C.; Friend, R. H.; Holmes, A. B. *Nature* **1993**, *365*, 628. (b) Strukelj, M.; Miller, T. M.; Papadimitrakopoulos, F.; Sun, S. *J. Am. Chem. Soc.* **1995**, *117*, 11976. (c) Ganstrom, M.; Inganas, O. *Appl. Phys. Lett.* **1996,** *68*, 147.

(9) (a) Berlman, I. B. *Handbook of Fluorescence Spectra of Aromatic Molecules*; Academic Press: New York, 1965. (b) Ott, D. G.; Hayes, F. N.; Hansbury, E.; Kerr, V. N. *J. Am. Chem. Soc.* **1957**, *79*, 5448. (c) Birks, J. B. *Photophysics of Aromatic Molecules*; Wiley-Interscience: London, 1970.

(10) (a) Kuhn, H. *Thin Solid Films* **1983**, *99*, 1. (b) Kuhn, H. *J. Photochem.* **1979**, *10*, 111. (c) Kuhn, H. *Pure Appl. Chem.* **1981**, *53*, 2105. (d) Mobius, D. *Acc. Chem. Res* **1981**, *14*, 2105.

(11) (a) Baker, S.; Petty, M. C.; Roberts, G. G.; Twigg, M. V. *Thin Solid Films* **1983**, *99*, 53. (b) Jones, R.; Tredgold, R. H.; Hodge, P. *Thin Solid Films* **1983**, *99*, 25. (c) Dutta, A. K.; Misra, T. N.; Pal, A. J. *J. Phys. Chem.* **1994**, *98*, 4365. (d) Dutta, A. K.; Misra, T. N.; Pal, A. J. *Langmuir* **1996**, *12*, 459. (e) Dutta, A. K.; Kamada, K.; Ohta, K. *Langmuir* **1996**, *12*, 4158. (f) Wistus, E.; Mukhtar, E.; Almgren, M.; Lundquist, S. E. *Langmuir* **1992,** *8*, 1366.

(12) (a) Ulman, A.; Scarnige, R. P. *Langmuir* **1992**, *8*, 894. (b) Verschuere, B.; Van der Auweraer, M.; De Schryver, F. C. *Thin Solid Films* **1994**, *244*, 995. (c) Angelova, A.; Van der Auweraer, M.; Ionov, R.; Vollhardt, D.; De Schryver, F. C. *Langmuir* **1995**, *11*, 3167.

(13) (a) Flament, C.; Gallet, F. *Thin Solid Films* **1994**, *244*, 1026. (b) Tsukruk, V. V.; Reneker, D. H.; Bliznyuk, V. N.; Kirstein, S.; Mohwald, H. *Thin Solid Films* **1994**, *244*, 763. (c) Facci, P.; Erokhin, V.; Nicolini, C. *Thin Solid Films* **1994**, *243*, 403. (d) Weiss, R. M.; McConell, M. *Nature* **1984**, *310*, 47.

(14) (a) Dutta, A. K.; Misra, T. N.; Pal, A. J. *J. Phys. Chem.* **1994**, *98*, 12844. (b) Dutta, A. K. *J. Phys. Chem.* **1995**, *99*, 14758. (c) Sakuhara, T.; Nakahara, H.; Fukuda, K. *Thin Solid Films* **1988**, *159*, 345.

(15) (a) Schoeler, U.; Tews, K. H.; Kuhn, H. *J. Chem. Phys.* **1974,** *61*, 5009. (b) Nakahara, H.; Nakayama, J.; Hoshino, M.; Fukuda, F. *Thin Solid Films* **1988**, *160*, 87.

(16) (a) Hall, R. A.; Thistlewaite, P. J.; Grieser, F. *Langmuir* **1993**, *9*, 2128. (b) Daniel, M. F.; Lettington, O. C.; Small, S. M. *Thin Solid Films* **1983**, *99*, 61. (c) Daniel, M. F.; Lettington, O. C.; Small, *Mol. Cryst. Liq. Cryst.* **1983**, *96*, 373. (d) de Mul, M. N. G.; Mann, J. A. *Langmuir* **1995**, *11*, 3292. (e) de Mul, M. N. G.; Mann, J. A. *Langmuir* **1994**, *10*, 2311. (f) Friendenberg, M. C.; Fuller, G. G.; Frank, C. W.; Robertson, C. R. *Langmuir* **1994,** *10*, 1251. (g) Xue, J.; Jung, C. S.; Kim, M. W. *Phys. Rev. Lett.* **1992**, *69*, 474.

(17) (a) Lavgine, P.; Trancrede, P.; Lamarche, F.; Grandbois, M.; Salesse, C. *Thin Solid Films* **1994**, *242*, 229. (b) Takeda, F.; Matsumoto, M.; Takenaka, T.; Fujiyoshi, Y. *J. Colloid Interface Sci.* **1983**, *91*, 267. (c) Takeda, F.; Matsumoto, M.; Takenaka, T.; Fujiyoshi, Y. *J. Colloid Interface Sci.* **1981**, *84*, 220. (d) Malcolm, B. R. *J. Colloid Interface Sci.* **1985**, *104*, 520. (e) Malcolm, B. R. *Biochem J.* **1968**, *110*, 733. (f) Malcolm, B. R. *Nature* **1962**, *195*, 901.

(18) (a) Pallas, N. R.; Pethica, B. A. *J. Chem. Soc., Faraday Trans. 1* **1987**, *83*, 585. (b) Moore, B. G.; Knobler, C. M.; Akamatsu, S.; Rondelez, F. *J. Phys. Chem.* **1990**, *94*, 4588.

(19) (a) Pallas, N. R.; Pethica, B. A. *Langmuir* **1985**, *1*, 509. (b) Bohanon, T. M.; Lin, B.; Shih, M. C.; Ice, G. E.; Dutta, P. *Phys. Rev.* **1990,** *B41,* 4846. (c) Lin, B.; Shih, M. C.; Ice, G. E.; Dutta, P. *Langmuir* **1990**, *6*, 1665. (d) Demel, R. A.; Joos, P. *Chem. Phys. Lipids* **1968**, *2*, 35.

(20) Kramarenko, S. F.; Tkachev, V. A.; Tolmachev, A. V.; Voronkina, N. I.; Afanasyeva, M. A.; Krainov, I. P. *Thin Solid Films* **1992**, *210/211*, 224.

(21) (a) Adamson, A. W. *Physical Chemistry of Surfaces*; Wiley-Interscience: New York, 1990. (b) Gaines, G. L., Jr. *J. Colloid Interface Sci.* **1966**, *21*, 315. (c) Gaines, G. L., Jr. *J. Chem. Phys.* **1978**, *69*, 924. (d) Ito, H.; Morton, T. H.; Vodyanoy, V. *Thin Solid Films* **1989,** *180*, 180. (e) Dorfler, H. D.; *Adv. Colloid Interface Sci.* **1990**, *31*, 1.

(22) (a) Gabriella, G.; Baglioni, P. *J. Colloid Interface Sci.* **1981**, *83*, 221. (b) Rettig, W.; Dorfler, H. D. *Mater. Sci. Forum*, **1988**, *25/26*, 577. (c) Pagano, A. E.; Gershfeld, N. C. *J. Phys. Chem.* **1972**, *76*, 1238. (d) Gabriella, G.; Maddii, A. *J. Colloid Interface Sci.* **1978**, *64*, 19. (e) Reis, H. E., Jr.; Walker, D. C. *J. Colloid Sci.* **1961**, *16*, 361. (f) Dorfler, H. D. *Adv. Colloid Interface Sci.* **1990**, *31*, 1.

(23) (a) Overbeck, G. A.; Honig, D.; Mobius, D. *Langmuir* **1993**, *9*, 555. (b) Henon, S.; Meunier, *J. Rev. Sci. Instrum.* **1991**, *62*, 936. (c) Honig,

D.; Mobius, D. *J. Phys. Chem.* **1991**, *95*, 4590. (d) Honig, D.; Mobius, D. *Thin Solid Films* **1992,** *210/211*, 64. (e) Honig, D.; Overbeck, G. A.; Mobius, D. *Adv. Mater.* **1992**, *4*, 419.

(24) (a) McRae, E. G.; Kasha, M. *Physical Processes in Radiation Biology*; Augenstein, L., Mason, R., Rosenberg, B., Eds.; Academic Press: New York, London, 1964; p 23. (b) McRae, E. G.; Kasha, M. *J. Chem. Phys.* **1958**, *28*, 721. (c) Kasha, M.; Rawls, H. R.; El-Bayoumi, M. A. *Pure Appl. Chem.* **1965**, *11*, 37. (d) Jelly, E. E. *Nature* **1936**, *138*, 1009. (e) Schiebe, G. *Angew. Chem.* **1936**, *49*, 563. (f) Czikkely, V.; Forsterling, H. D.; Kuhn, H. *Chem. Phys. Lett.* **1970**, *6*, 11. (g) Czikkely, V.; Forsterling, H. D.; Kuhn, H. *Chem. Phys. Lett.* **1970**, *6*, 207. (h) West, W.; Caroll, B. M. *J. Chem. Phys.* **1951**, *19*, 417. (i) Van der Auweraer, M.; Verschuere, B.; De Schryver, F. C. *Langmuir* **1988**, *4*, 583. (j) Miyata, A.; Heard, D.; Unuma, Y.; Higashigaki, Y. *Thin Solid Films* **1992**, *210/211* 175.

(25) Turro, N. J. *In Modern Molecular Photochemistry*; The Benjamin/Cummings Publishing Co. Inc.: London, 1936.

(26) (a) Anderson, R.; Davidson, K.; McInally, I.; Soutar, I.; Birch, D. J. S.; Imhof, R. E. *J. Photochem. Photobiol., A* **1988**, *45*, 123. (b) Berlman, I. B. *J. Chem. Phys.* **1961**, *34*, 1083. (c) Agbaria, R. A.; Gill, D. *J. Chem. Phys.* **1988**, *92*, 1052. (d) Agbaria, R. A.; Gill, D. *J. Photochem. Photobiol., A* **1995**, *78*, 161. (e) Horrocks, D. L. *J. Chem. Phys.* **1969**, *50*, 4962.

(27) (a) Lami, H.; Laustriat, G. *J. Chem. Phys.* **1968**, *48*, 1832. (b) Horrocks, D. L. *J. Chem. Phys.* **1967**, *47*, 3089.

(28) (a) Baudor, J. L.; Callieu, H.; Yelon, W. B. *Acta Crystallogr.* **1977**, *33B*, 1973. (b) Baudor, J. L.; Delugard, Y.; Rivet, P. *Acta Crystallogr.* **1978**, *34B*, 625. (c) Reitveld, H. M.; Maslen, E. N.; Clews, C. T. B. *Acta Crystallogr.* **1970** *26B*, 693. (d) Saito, K.; Atake, T.; Chihara, H. J. *Bull. Chem. Soc. Jpn.* **1988**, *61*, 2327. (e) Saitoh, H.; Saito, K.; Yamamoto, Y.; Matsumyama, H.; Kikuchi, K.; Ikemoto, I. *Solid State Commun.* **1994**, *91*, 89. (f) Saitoh, K.; Yamammura, Y.; Matsuyama, H.; Kikuchi, K.; Ikemoto, I. *Solid State Commun.* **1994**, *92*, 495.

(29) Doroshenko, A. O.; Kirichenko, A. V.; Mitina, V. G.; Ponomaryov, O. A. *J. Photochem. Photbiol., A* **1996**, *94*, 15.

(30) (a) Zhen, Z.; Tung, C.; *J. Photochem. Photobiol., A* **1992**, *68*, 247. (b) Ruban, A. V.; Horton, P. Young, A. J. *J. Photochem. Photobiol., A* **1993**, *21*, 229.

(31) Weinberger, R.; ClineLove, L. J. *Spectrochim. Acta* **1984**, *40A*, 49.

(32) (a) Uchida, K.; Sato, S.; Takahashi, Y. *J. Lumin* **1991**, *48/49* 377. (b) Willams, J. O. *Chem. Phys. Lett.* **1976**, *42*, 171. (c) Swiathoski, G.; Menzel, R.; Rapp, W. *J. Lumin.* **1987**, *37*, 183.

(33) Lakowicz, J. R. In *Principles of Fluorescence Spectroscopy*; Plenum Press: New York, 1983; Chapter 5.